Determination of graphene work function and graphene-insulator-semiconductor band alignment by internal photoemission spectroscopy

Rusen Yan,[1,2,a)] Qin Zhang,[1,2] Wei Li,[1,3] Irene Calizo,[1] Tian Shen,[1,4] Curt A. Richter,[1] Angela R. Hight-Walker,[1] Xuelei Liang,[3] Alan Seabaugh,[2] Debdeep Jena,[2] Huili Grace Xing,[2] David J. Gundlach,[1] and N. V. Nguyen[1,b)]
[1]*Semiconductor and Dimensional Metrology Division, National Institute of Standards and Technology, Gaithersburg, Maryland 20899, USA*
[2]*Department of Electrical Engineering, University of Notre Dame, Notre Dame, Indiana 46556, USA*
[3]*Key Laboratory for the Physics and Chemistry of Nano Devices, Peking University, Beijing, China*
[4]*Department of Physics, Purdue University, West Lafayette, Indiana 47907, USA*

(Received 30 May 2012; accepted 22 June 2012; published online 11 July 2012)

We determined the band alignment of a graphene-insulator-semiconductor structure using internal photoemission spectroscopy. From the flatband voltage and Dirac voltage, we infer a 4.6 $\times$ 10^{11} cm^{-2} negative extrinsic charge present on the graphene surface. Also, we extract the graphene work function to be 4.56 eV, in excellent agreement with theoretical and experimental values in literature. Electron and hole injection from heavily doped p-type silicon (Si) are both observed. The barrier height from the top of the valence band of Si to the bottom of the conduction band of silicon dioxide (SiO_2) is found to be 4.3 eV. The small optical absorption in graphene makes it a good transparent contact to enable the direct observation of hole injection from Si to graphene. The barrier height for holes escaping from the bottom of Si conduction band to the top of SiO_2 valence band is found to be 4.6 eV. © *2012 American Institute of Physics*. [http://dx.doi.org/10.1063/1.4734955]

Graphene, an attractive two-dimensional (2D) carbon material, has gained intensive research interest due to its unique physical and optical properties.[1–4] Researchers have proposed a variety of promising applications using these thin carbon films, such as terahertz wave modulators,[5,6] field-effect tunneling transistors,[7] etc. The performances of these device architectures are critically dependent on how the graphene-insulator-graphene (or semiconductor) (GIG or GIS) electronic bands align with each other. Specifically, under various gate voltages, their proper operations are a strong function of the relative position of Fermi levels on top and bottom conductive layers. However, no detailed study of band alignment in such GIG or GIS structures is reported to date. In this letter, we investigate the interfacial electronic properties of a graphene-oxide-silicon stack using internal photoemission (IPE) spectroscopy, which has been shown to be an accurate technique to characterize the band alignment of metal-oxide-semiconductor structures or heterojunctions.[8–10] Our study clearly shows a difference of flatband voltage from Dirac voltage in the device due to the presence of extrinsic charges at the silicon-dioxide (SiO_2)/graphene interface or possibly adsorbed on the graphene surface.

The sample structure and the measurement configuration are schematically shown in Fig. 1(a). A large-area single layer graphene film grown by chemical vapour deposition (CVD) was transferred to a degenerately doped p-type silicon (Si) substrate with a 10 nm thick thermal SiO_2 layer.[11,12] To circumvent photoemission from the metal into graphene, a thick layer 180 nm of evaporated Al is used. The graphene channel is patterned using oxygen plasma etching. A representative Raman spectra ($\lambda_{ex} = 514$ nm) of the graphene in our device is shown in Fig. 1(b), which confirms it is monolayer graphene.[13] Considering the fact that 10 nm SiO_2 does not allow distinctive visibility of the graphene flake,[14] we also show a spatial map of Raman G peak intensity at the edge of our device in Fig. 1(d) with its optical image shown in Fig. 1(c). The IPE measurement system mainly consists of a 150 W broadband Xenon light source and a quarter-meter Czerny Turner monochromator to tune the incident light with photon energy ranging from 1.5 eV to 5.5 eV. The photocurrent (I_{ph}) flowing between graphene and Si is recorded by an electrometer as a function of photon energy ($h\upsilon$) with various externally applied voltages (V_{gs}). The corresponding quantum yield (Y) is calculated as the ratio of I_{ph} to the incident light flux (P). More details about IPE setup can be found in Ref. 15.

Fig. 2(a) shows I_{ph} vs $h\upsilon$ as gate voltage V_{gs} varies from 0 V to 1 V in step of 0.1 V with graphene grounded. It can be seen that the photocurrent switches from negative to positive at a certain gate voltage, defined as the flatband voltage (V_{fb}), at which the electric field in the thin oxide and thus current both reach zero. To determine V_{fb} accurately, in Fig. 2(b), we have plotted I_{ph} vs V_{gs} for photon energy larger than 5 eV and their linear fits yield $V_{fb} = (0.56 \pm 0.05)$ V at $I_{ph} = 0$. As will be shown in the following, the negative and positive currents are in fact the electron and hole injection from Si into graphene, respectively. Under illumination from the top of the device, electron-hole pairs are generated at the Si/SiO_2 interface. When $V_{gs} < V_{fb}$, electrons are photostimulated from the Si valence band to energy levels higher than the bottom of the oxide conduction band and driven by the electric field across the oxide into the graphene, thus producing the negative current. On the other hand, when $V_{gs} > V_{fb}$, the reversed electric field in the thin oxide drives holes

a)Electronic mail: ryan1@nd.edu.
b)Electronic mail: nhan.nguyen@nist.gov.

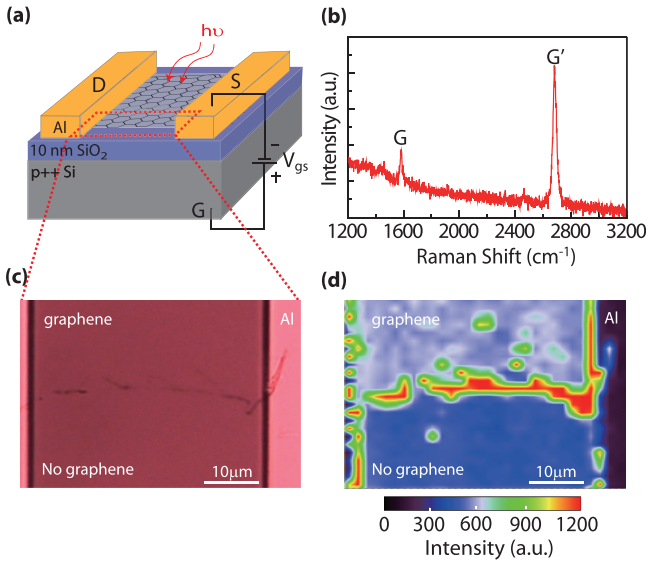

FIG. 1. (a) Device structure. A gate voltage V_{gs} is applied between graphene and the p^{++} Si substrate with the aluminum top contact grounded. (b) Representative Raman spectrum collected on our device. The ratio of the G and G' peaks confirms that it is monolayer graphene. (c) and (d) Optical and corresponding Raman mapping image of the G peak intensity near the edge of the device. The contrast in (d) identifies the region with and without graphene which is invisible in the optical image.

photostimulated to the SiO_2 valence band into the graphene, which contributes to the positive current. Because the optical absorption in graphene is known to be small,[16] photostimulation from the graphene Fermi level to the SiO_2 conduction band is assumed to be negligible, thus the positive current is attributed to hole emission from Si. In the following, both electron and hole barrier heights on Si side will be determined.

The IPE quantum yield near the barrier threshold can be expressed as[17]

$$Y^{1/p} = A(h\upsilon - \phi), \tag{1}$$

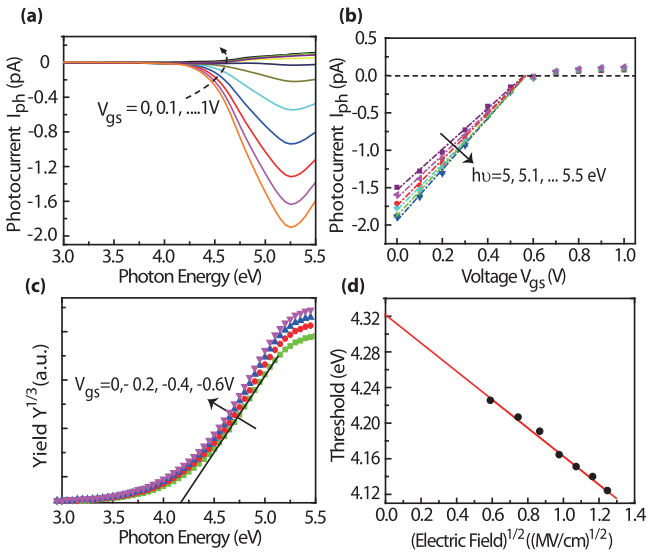

FIG. 2. (a) Photocurrent as a function of incident photon energy and gate bias. (b) Photocurrent as a function of gate voltage. (c) Cubic root of yield $Y^{1/3}$ for negative current under different gate voltages. (d) Schottky plot of negative current (electron injection). The barrier height linearly relates to $E^{1/2}$. The measurement system description and data analysis are discussed in Ref. 15

where A is a constant, $p = 3$ for Si,[17] and ϕ is the threshold, i.e., the barrier height from the top of the Si valence band to the bottom of the SiO_2 conduction band for the case of electron emission. According to Eq. (1), we can obtain the spectral threshold through the linear extrapolation to zero yield of the $Y^{1/3}$ vs $h\upsilon$ characteristics as shown in Fig. 2(c). Due to the Coulomb interaction between the electron photoemitted into the oxide with the charge of the polarized emitter,[18] the barrier heights extracted show a linear relation to the square root of electric field in the oxide as exhibited in the Schottky plot in Fig. 2(d). The linear extrapolation to zero field gives a zero-field barrier height ϕ_0^e of 4.3 eV. Similar barrier height determination is performed for positive photocurrent as well, i.e., hole injection. As a result, the corresponding barrier height ϕ_0^h from the bottom of Si conduction band to the top of SiO_2 valence band is extracted to be 4.6 eV. With these values, we can estimate the bandgap of thin SiO_2 to be approximately 7.9 eV, following $E_g^{SiO_2} = \phi_0^e + \phi_0^h - E_g^{Si}$,[19] where ϕ_0^e and ϕ_0^h are barrier heights encountered by electrons and holes, respectively. This result is in close agreement with the value extracted from ellipsometric data taken on the same sample, from which the Tauc plot[20] yields $E_g^{SiO_2} = 8.0$ eV.

To correlate the IPE results with electric charges on the graphene side, we also performed $I_d - V_{gs}$ measurements on the same device. The $I_d - V_{gs}$ characteristic shown in the inset of Fig. 3 suggest a Dirac voltage (V_{Dirac}) of 0.84 V, which differs from V_{fb} measured by IPE by (0.28 ± 0.05) V. This discrepancy provides a direct evidence of the existence of extrinsic charges (n_{ex}, charge density per unit area) on the graphene side of the device. As being one-atom thick, graphene is sensitive to the surface condition.[21,22] Under the flatband condition ($V_{gs} = V_{fb}$), there is no electric field inside the oxide, which means, n_t, the total charge density per unit area on the graphene side, and n_s, the total mobile charge concentration in graphene, have to satisfy the condition $n_t = n_s + n_{ex} = 0$, that is, $n_{ex} = -n_s$. Therefore, with the departure of V_{Dirac} from V_{fb}, we can estimate n_{ex} by examining n_s. We assume n_{ex} is a fixed charge concentration

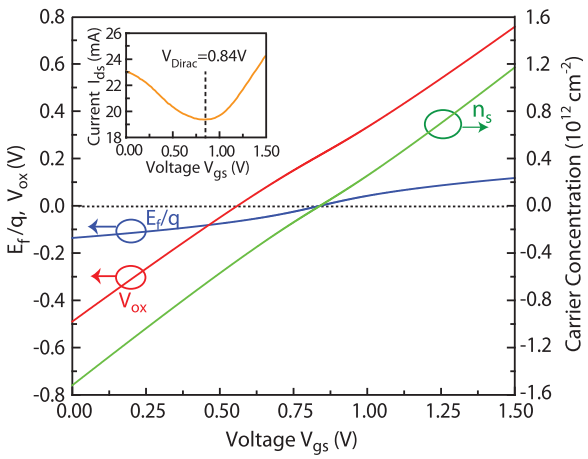

FIG. 3. Calculated voltage drop across the oxide (red) and the difference between graphene Fermi level and its Dirac point (blue) as a function of gate voltage V_{gs}. The carrier concentration in graphene (green) where negative and positive values, respectively, relates to hole and electron as majority carriers. The inset shows the $I_d - V_{gs}$ characteristic of the device. Minimum conductivity is reached at $V_{gs} = 0.84$ V.

independent of the graphene Fermi level (E_f). The application of a gate voltage V_{gs} leads to the variation of carrier concentration and thus the shift of Fermi level in graphene, which can be characterized by the following relation:[23]

$$V_{gs} - V_{Dirac} = \frac{E_f}{q} + \frac{n_s q}{C_{ox}}, \tag{2}$$

where E_f is the Fermi level in graphene, $C_{ox} = \epsilon/d = 0.345\,\mu\text{F/cm}^2$ (ϵ: dielectric constant; d: oxide thickness) is the gate oxide capacitance per unit area, and q is electron charge. In Eq. (2), the carrier concentration is given by[24]

$$\begin{aligned} n_s &= n_0 - p_0 \\ &= \frac{2}{\pi}\left(\frac{kT}{\hbar|v_f|}\right)^2 F_1(+\eta) - \frac{2}{\pi}\left(\frac{kT}{\hbar|v_f|}\right)^2 F_1(-\eta), \end{aligned} \tag{3}$$

where $F_j(\eta)$ is Fermi-Dirac integral with $j = 1$ and $\eta = E_f/kT$, k is Boltzmann constant, $T = 300\,\text{K}$ is the absolute temperature, $\hbar$ is Planck's constant divided by 2π, and $|v_f| = 10^6\,\text{m/s}$ is the Fermi velocity. Note that $n_s > 0$ and $n_s < 0$ correspond to the cases of electron and hole as the majority carrier in graphene, respectively. Here, we choose to use the temperature dependent formula instead of the 0 K approximation that is widely adopted in the literature since the 0 K approximation introduces an error of 25% at $|E_f| = 0.08\,\text{eV}$ in terms of n_s, only with an acceptable error of <5% when $|E_f| > 0.2\,\text{eV}$. Using Eqs. (2) and (3), in Fig. 3, we plot E_f/q (blue), n_s (green), and the net voltage over the oxide V_{ox} (red). It can be seen that at $V_{gs} = V_{fb} = (0.56 \pm 0.05)\,\text{V}$, the Fermi level E_f in graphene is about (0.08 ± 0.01) eV below its Dirac point, which corresponds to the hole concentration $n_s = (4.6 \pm 0.8) \times 10^{11}\,\text{cm}^{-2}$. To maintain the flatband condition, there must be the same amount of negative charges externally induced by the environment to compensate these holes. Therefore, $n_{ex} = |n_s| = (4.6 \pm 0.8) \times 10^{11}\,\text{cm}^{-2}$.

Most strikingly, the measurement of all these quantities, ϕ_0^e, V_{fb}, and V_{Dirac} allows us to accurately depict the band alignment in the graphene-SiO_2-Si structure. In Figs. 4(a) and 4(b), we show the band diagram when $V_{gs} = V_{fb}$ and $V_{gs} = 0$, respectively, where $\phi_0^e = 4.3\,\text{eV}$ is the barrier height from the top of Si valence band to the bottom of SiO_2 conduction band; $qV_{gs} = qV_{fb} = (0.56 \pm 0.05)\,\text{eV}$ is the Fermi level difference between graphene and p^{++} Si under the flatband condition; $E_f = (0.08 \pm 0.01)$ eV is how far the Fermi level in graphene departs from its Dirac point. The height from the graphene Dirac point to the conduction band bottom of SiO_2 is calculated to be (3.66 ± 0.04) eV. By employing the well-known 0.9 eV electron affinity of SiO_2,[25] the work function of intrinsic graphene is extracted to be (4.56 ± 0.04) eV, in excellent agreement with values reported previously.[26–29]

In summary, we have determined the band offsets in a graphene-SiO_2-Si structure by employing IPE in conjunction with $I_d - V_{gs}$ measurements. These results establish the work function of intrinsic graphene to be $(4.56 \pm 0.04)\,\text{eV}$, in good agreement with previous estimations and measurements. Furthermore, they allow one to extract extrinsic doping, which in this sample is found to have a density of

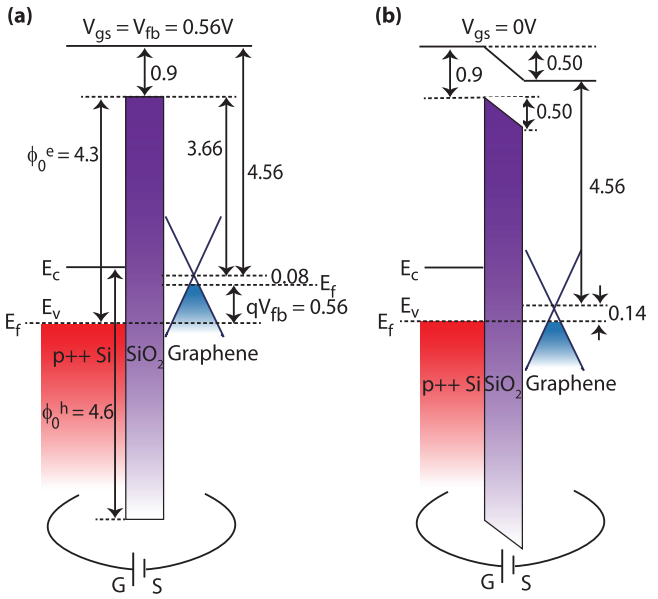

FIG. 4. Band diagrams when (a) $V_{gs} = V_{fb}$ and (b) $V_{gs} = 0\,\text{V}$. All the numbers labeled in the figure are in units of eV.

$(4.6 \pm 0.8) \times 10^{11}\,\text{cm}^{-2}$ negative charges based on the discrepancy between the Dirac voltage and flatband voltage. While not discussed in detail, we show that graphene can be used as an ideal transparent contact for IPE measurements to enabling the observation of hole injection. We believe that the key band structure reported here will pave the way for future studies on electric and optical devices utilizing a GIG (or GIS) configuration.

The authors gratefully acknowledge the support of the NIST Semiconductor and Dimensional Metrology Division and the Nanoelectronics Research Initiative through the Midwest Institute for Nanoelectronics Discovery (MIND).

[1]K. S. Novoselov, A. K. Geim, S. V. Morozov, D. Jiang, Y. Zhang, S. V. Dubonos, I. V. Grigorieva, and A. A. Firsov, Science **306**, 666 (2004).
[2]K. S. Novoselov, A. K. Geim, S. V. Morozov, D. Jiang, M. I. Katsnelson, I. V. Grigorieva, S. V. Dubonos, and A. A. Firsov, Nature **438**, 197 (2005).
[3]F. Wang, Y. Zhang, C. Tian, C. Girit, A. Zettl, M. Crommie, and Y. R. Shen, Science **320**, 206 (2008).
[4]A. Vakil and N. Engheta, Science **332**, 1291 (2011).
[5]B. Sensale-Rodriguez, T. Fang, R. Yan, M. M. Kelly, D. Jena, L. Liu, and H. Xing, Appl. Phys. Lett. **99**, 113104 (2011).
[6]B. Sensale-Rodriguez, R. Yan, M. M. Kelly, T. Fang, K. Tahy, W. S. Hwang, D. Jena, L. Liu, and H. Xing, Nat. Commun. **3**, 780 (2012).
[7]L. Britnell, R. V. Gorbachev, R. Jalil, B. D. Belle, F. Schedin, A. Mishchenko, T. Georgiou, M. I. Katsnelson, L. Eaves, S. V. Morozov, N. M. R. Peres, J. Leist, A. K. Geim, K. S. Novoselov, and L. A. Ponomarenko, Science **335**, 947 (2012).
[8]N. V. Nguyen, O. A. Kirillov, W. Jiang, W. Wang, J. S. Suehle, P. D. Ye, Y. Xuan, N. Goel, K. W. Choi, W. Tsai, and S. Sayan, Appl. Phys. Lett. **93**, 082105 (2008).
[9]V. V. Afanasev and A. Stesmans, J. Appl. Phys. **102**, 081301 (2007).
[10]Q. Zhang, G. Zhou, H. Xing, A. C. Seabaugh, K. Xu, H. Sio, O. A. Kirillov, C. A. Richter, and N. V. Nguyen, Appl. Phys. Lett. **100**, 102104 (2012).
[11]X. Li, W. Cai, J. An, S. Kim, J. Nah, D. Yang, R. Piner, A. Velamakanni, I. Jung, E. Tutuc, S. K. Banerjee, L. Colombo, and R. S. Ruoff, Science **324**, 1312 (2009).
[12]X. Liang, B. Sperling, I. Calizo, G. Cheng, C. Hacker, Q. Zhang, Y. Obeng, K. Yan, H. Peng, Q. Li, X. Zhu, H. Yuan, A. Walker, Z. Liu, L. Peng, and C. Richter, ACS Nano **5**, 9144 (2011).

[13]A. Reina, X. Jia, J. Ho, D. Nezich, H. Son, V. Bulovic, M. S. Dresselhaus, and J. Kong, Nano. Lett. **9**, 30–35 (2009).
[14]P. Blake, E. W. Hill, A. H. Castro Neto, K. S. Novoselov, D. Jiang, R. Yang, T. J. Booth, and A. K. Geim, Appl. Phys. Lett. **91**, 063124 (2007).
[15]N. V. Nguyen, O. A. Kirillov, and J. S. Suehle, Thin Solid Films **219**, 2811 (2011).
[16]R. R. Nair, P. Blake, A. N. Grigorenko, K. S. Novoselov, T. J. Booth, T. Stauber, N. M. R. Peres, and A. K. Geim, Science **320**, 1308 (2008).
[17]R. J. Powell, J. Appl. Phys. **41**, 2424 (1970).
[18]S. M. Sze and K. K. Ng, *Physics of Semiconductor Devices*, 3rd ed. (Wiley, New Jersey, 2007).
[19]V. K. Adamchuk and V. V. Afanas'ev, Prog. Surf. Sci. **41**, 111 (1992).
[20]N. V. Nguyen, S. Sayan, I. Levin, J. R. Ehrstein, I. J. R. Baumvol, C. Driemeier, C. Krug, L. Wielunski, P. Y. Hung, and A. Diebold, J. Vac. Sci. Technol A. **23**, 1706 (2005).
[21]K. Nomura and A. H. MacDonald, Phys. Rev. Lett. **98**, 076602 (2007).
[22]F. Schedin, A. K. Geim, S. V. Morozov, E. W. Hill, P. Blake, M. I. Katsnelson, and K. S. Novoselov, Nature Mater. **6**, 652 (2007).
[23]A. Das, S. Pisana, B. Chakraborty, S. Piscanec, S. K. Saha, U. V. Waghmare, K. S. Novoselov, H. R. Krishnamurthy, A. K. Geim, A. C. Ferrari, and A. K. Sood, Nat. Nanotechnol. **3**, 210 (2008).
[24]T. Fang, A. Konar, H. Xing, and D. Jena, Appl. Phys. Lett. **91**, 092109 (2007).
[25]R. Williams, Phys. Rev. **140**, A569 (1965).
[26]T. Filleter, K. V. Emtsev, Th. Seyller, and R. Bennewitz, Appl. Phys. Lett. **93**, 133117 (2008).
[27]S. S. Datta, D. R. Strachan, E. J. Mele, and A. T. C. Johnson, Nano. Lett. **9**, 7–11 (2009).
[28]T. Takahashi, H. Tokailin, and T. Sagawa, Phys. Rev. B **32**, 8317 (1985).
[29]Y. J. Yu, Y. Zhao, S. Ryu, L. E. Brus, K. S. Kim, and P. Kim, Nano. Lett. **9**, 3430 (2009).